SURFACE CHARACTERIZATION OF ANODICALLY TREATED β - TITANIUM ALLOY FOR BIOMEDICAL APPLICATIONS

R. Bhola[1], S. M. Bhola[2], B. Mishra[3], R. A. Ayers[4], D. L. Olson[5], T. Ohno[6]

[1]Department of Biologic Material Sciences,
[2]Department of Nuclear Engineering and Radiological Sciences,
University of Michigan, Ann Arbor, MI 48109 USA
[3–6]Department of Metallurgical & Materials Engineering,
Colorado School of Mines, Golden, CO 80401 USA, bhola.rahul@gmail.com, bholar@umich.edu

Introduction

The surface characteristics of an implantable material play an important role in governing the cellular response. The objective of modifying the surface characteristics of a biomaterial by means of a surface treatment, such as, ion implantation, sputter coating, thermal oxidation or anodic oxidation is to improve its corrosion resistance, wear properties as well as its biocompatibility [1]. Anodic oxidation is one of the commonly used methods that can be successfully used to enhance these properties for biomedical applications [2–7].

The study of the interface between a living cell and a biomaterial is crucial in understanding the mechanism of cellular adhesion. Parameters such as surface roughness, surface chemistry, oxide thickness and the presence of contaminants on the surface are known to affect this interface and subsequently the biological response both in-vivo and in-vitro [8–11]. Such an interface was investigated in-vitro by Davis et al. [12] and de Bruijn et al. [13] for conventional titanium alloys, where the interface formed comprised of a layer of Ca and P rich globular deposits, adjacent to the implant surface over which collagen fibers were deposited. A similar interface was also created in-vivo by others [14].

There has been an increasing interest over the last decade to develop alloys containing β stabilizing elements such as molybdenum, niobium, tantalum, zirconium that can improve the alloy strength and lower the modulus mismatch between the ductile bone and the comparatively brittle implant material, thus minimizing the stress shielding [15–20].

Ti15Mo alloy is a metastable β alloy whose basic metallurgy, mechanical and corrosion resistance properties have been thoroughly described in the metallurgical literature, especially its biocompatible advantages [21–23]. Ti15Mo alloy has a body centered cubic β microstructure with a higher strength over α and α+β alloys. It has low values of elastic modulus and stiffness which makes it beneficial for dental applications.

The work described here is part of a study in which Ti15Mo alloy was surface modified by anodic oxidation at 1 V in phosphate buffer saline solution and characterized for its cellular response and surface chemistry. The investigation was also performed for the mixed Ti6Al4V and the α Ti2 alloys for comparison. The surface modified alloys have been characterized for their corrosion behavior at various anodic potentials in our previous studies [24–25]. A value of 1 V as the anodization potential in the passivation range was chosen since it has been shown by Black that the potential value of a metallic biomaterial may generically vary up to 1.2 V vs SCE in the human body [26].

Experimental

Materials Preparation

Titanium alloy grades, Ti15Mo (0.05%C, 0.1%Fe, 0.015%H, 0.01%N, 0.15%O, 15%Mo & 84.67%Ti), Ti6Al4V (0.1%C, 0.2%Fe, 0.015%H, 0.03%N, 0.2%O, 6%Al, 4%V & 89.45%Ti) and Ti2 (0.1%C, 0.3%Fe, 0.015%H, 0.03%N, 0.25%O & 99.30%Ti), were used for the present investigation. Available cuboidal and cylindrical rods were machined to cylindrical samples of 5 mm in diameter and 5 mm in height with a hole 2 mm deep on one of the flat faces with a tap and drill #3-48. The hole was drilled to attach the specimens to the electrode holder in order to carry out the electrochemical anodization of the samples at 1 V. The exposed surface of the specimens was finished and polished with different grades of SiC grit papers (up to 2400 grit) and polished using a diamond abrasive wheel, washed with double distilled water and acetone.

Phosphate buffer saline solution (0.137M sodium chloride, 0.0027M potassium chloride and 0.01M phosphate buffer) of pH 7.4 was used to carry out the electrochemical anodization at 1V for all alloys.

© Bhola R., Bhola S. M., Mishra B., Ayers R.A., Olson D.L., Ohno T., Электронная обработка материалов, 2011, **47**(4), 75–82.

Measurements

Microstructure

The metal specimens were degreased, dried and mounted in bakelite resin. Mechanical grinding was done with SiC papers on a water cooled grinding stage up to paper 1800. Polishing was performed using gradually decreasing sizes of diamond abrasive from 6 μm to 1 μm and finally using a fine grained Al_2O_3 (with decreasing particle size from 0.5 μm to 0.25 μm) and cold saturated hydrous oxalic acid suspension on a short circular velvet cloth. The specimens were washed in de-ionized water and ethanol and air dried before etching. A universal etchant commonly known as the Kroll's reagent which is a hydrous solution comprising of 2 ml HF (40% conc.) and 6 ml HNO_3 (65% conc.) in 100 ml H_2O (de-ionized) was used for etching. The microstructure obtained was determined using optical microscopy.

Osteoblast Cell Culturing

Osteoblast cell count and morphology measurements were performed on all the anodized samples after immersing them in culture media containing human fetal osteoblast cells (derived from the human fetal osteoblast cell line: hFOB 1.19 ATCC, CRL11372) in a poly-styrene cell culture plate for 28 days at 37 °C. The procedure for cell culturing and counting has been described in another study [27]. All samples were sterilized in separately packed sterile containers using wet heat sterilization in an autoclave at 121°C at 15 psi for 15 minutes prior to immersion.

X-ray Photoelectron Spectroscopy (XPS)

Surrogate samples prepared for XPS characterization were exposed to human fetal osteoblast cells in a similar manner, as discussed above, for a period of 28 days at 37°C. They were then removed from the culture media, washed with trypsin (to remove the cells) and de-ionized water and ethanol before drying. XPS characterization was performed on the dried samples using a Kratos HSi system with an Al K_α monochromatic source. Surface profiling was performed with a MiniBeam I ion gun with 4 keV argon ions and an emission current of 10 mA. The rate of surface removal via sputtering was 3nm/min on a standard thermally oxidized Si wafer. The estimated amount of material removed assumed a similar sputter removal rate and lateral uniformity. Since sputter rates vary greatly and the passivating layer was partly covered by impurities, the stated amounts removed are the only guidelines.

Results and Discussion

The microstructure for Ti15Mo alloy can be observed in the SEM micrograph shown in Fig. 1. It primarily consists of large equiaxed grains of the β phase. Only a very small volume fraction of grain boundary α phase is present in the microstructure. The α laths formed during alloy aging nucleate within the interior of the grains and along the grain boundaries and are visible at higher magnifications. Growth and annealing twins are also visible in the micrograph.

The Ti6Al4V alloy is composed of equi-axed α grains, along with a lamellar α and β bimodal microstructure, as shown in Fig. 2. The α phase is a hexagonal close-packed (hcp) structure and is the stable phase at room temperature. The β phase is a body centered cubic (bcc) structure and is metastable below the β transus temperature. For this reason, the β phase is known to undergo a strain-induced phase change to the more stable α phase under certain conditions.

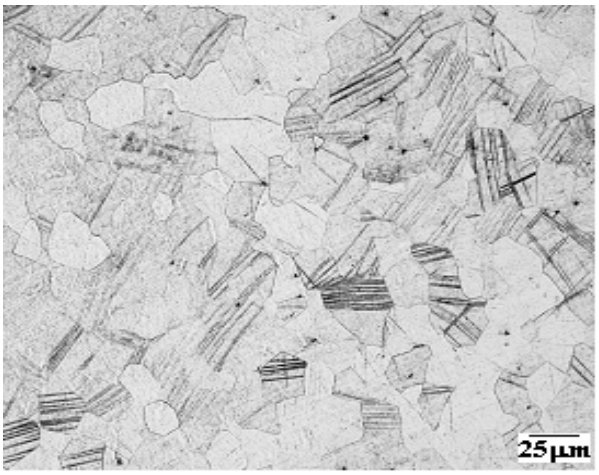

Fig. 1. Microstructure of β Ti15Mo alloy

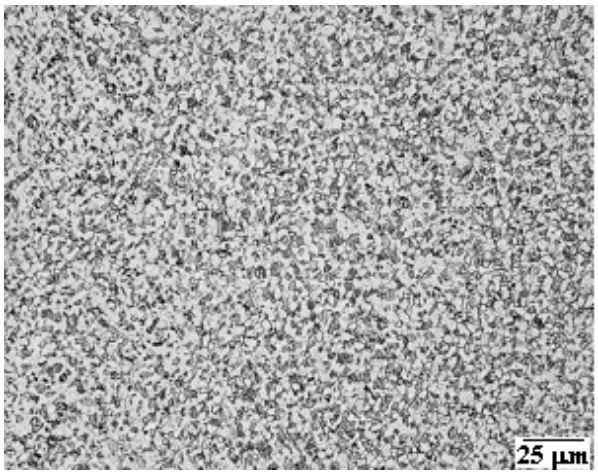

Fig. 2. Microstructure of α+β Ti6Al4V alloy

The microstructure for Ti2 alloy, as shown in Fig. 3, mainly consists of the fine α phase (hcp) dipersed throughout the alloy matrix.

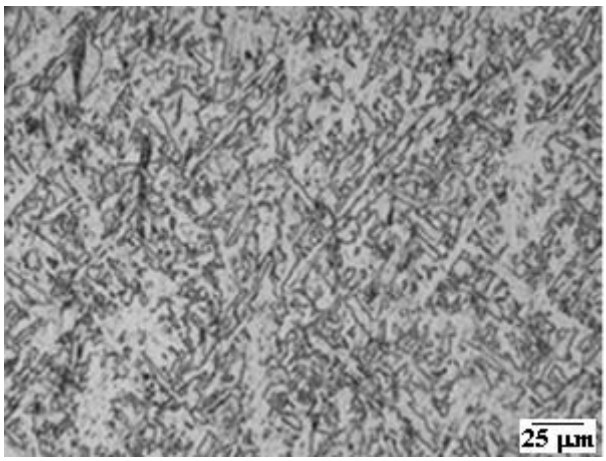

Fig. 3. Microstructure of α Ti2 alloy

Fig. 4 shows the cell counts for the osteoblasts attached over the anodized titanium alloy specimens at 37 °C. The cell counts follow an order Ti15Mo > Ti2 > Ti6Al4V. This implies that the cell attachment favors the β alloy followed by the α and the mixed alloys. Furthermore, in our previous study [27], the osteoblasts appeared elongated, stretched with a clear nucleus and dendrites connecting each other over the β alloys; dark, elongated and unhealthy with a compressed nucleus over the mixed alloy and dark, elongated and stretched with a clear nucleus and fewer dendritic connections over the α alloys. It was also found that Ti6Al4V alloy produced leaching of Al. Toxicity of Al ions has been widely reported [28–31] and can be detrimental to the biological performance of an implant. The low cell count values and an unhealthy morphology of osteoblasts for Ti6Al4V alloy, compared to those for Ti2 and Ti15Mo, can be due to the toxic effects of Al ions leached into the solution.

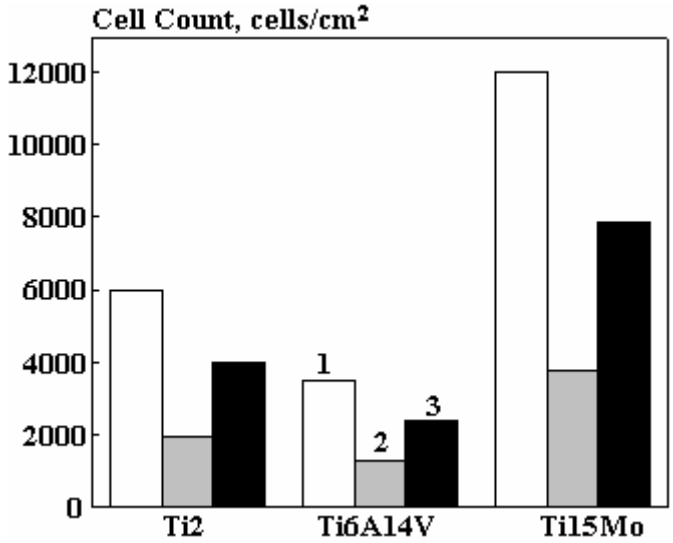

Fig. 4. Osteoblast cell counts for titanium alloys. 1 – 100 micron mesh; 2 – 400 micron mesh; 3 – Average

Fig. 5 (*a-c*) shows the XPS standard wide angle scans for the anodized alloy specimens.

The surface shows Na, K, P, Ca as well as trace amounts of Si, N and Cl. These ions were not removed by ion etching and are likely to represent the thick but non-uniform islands remaining from the evaporating culture solution.

The Ti2 alloy shows the presence of primarily TiO_2, with a Ti $2p_{3/2}$ primary peak at 459 eV, in Fig. 5,*a*. The exposed surface was majorly TiO_2, with small contributions from lower oxidation states and metallic titanium. The presence of the metallic titanium indicates that the passivating TiO_2 layer is sufficiently thin that photoelectrons from the underlying substrate can penetrate. The presence of the sub-oxides indicates that a graded composition exists.

Sputtering resulted in a spectrum that showed larger amounts of lower oxidation states, until only metallic titanium was observed as Ti $2p_{1/2}$ centered at 454.1 eV, after the removal of ~18 nm of material.

Oxides of intermediate oxidation states were present with binding energies (BE) between the metal and +4 oxidation state.

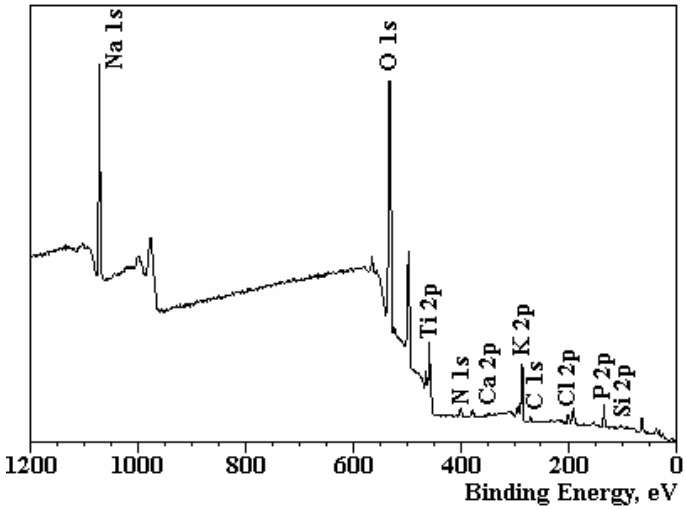

Ti2

a

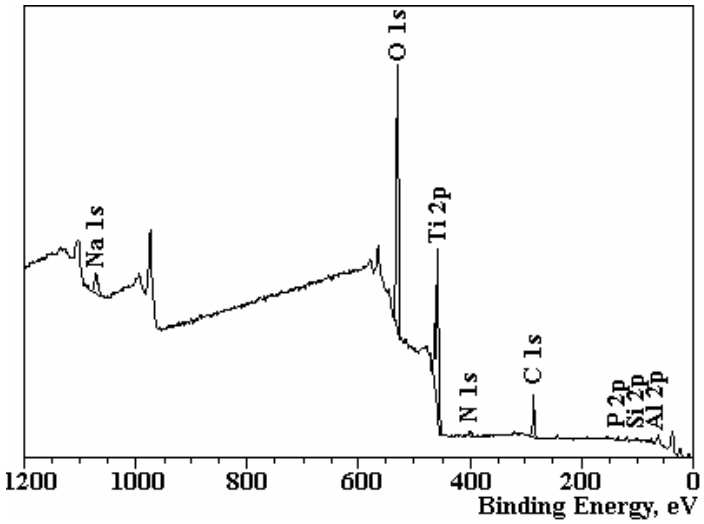

Ti6Al4V

b

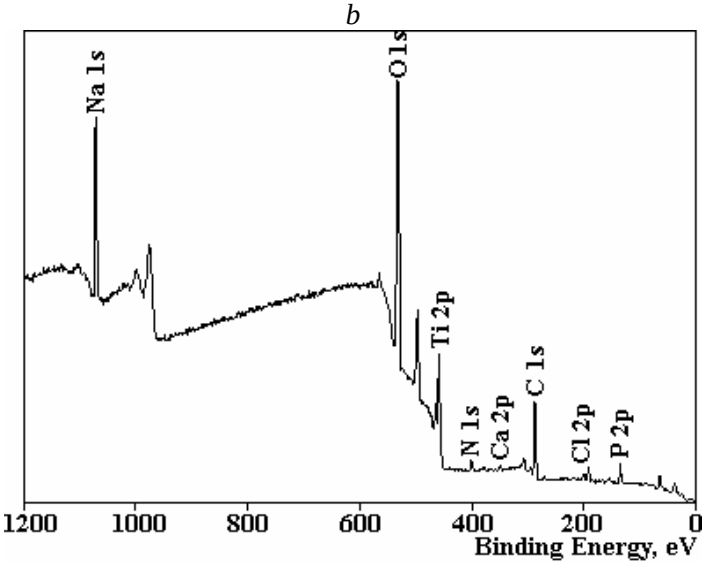

Ti15Mo

c

Fig. 5. (a–c). XPS standard wide angle scans for titanium alloys

Fig. 5,*b* shows the wide angle scan for Ti6Al4V alloy. The spectrum was predominately TiO_2, with smaller contributions from the sub-oxides and the metal. Vanadium and iron were not detected on the surface while aluminum was present in an oxidation state similar to the Al_2O_3, with a BE for the Al 2p of 75.7 eV.

After removal of 10 nm of material, both vanadium and aluminum in metallic states were visible, although aluminum was primarily in the +3 oxidation state. Approximately 50% of titanium was present as TiO_2 and sub-oxides and remaining as metallic Ti. After removal of ~30 nm of material, only metallic titanium and vanadium were present, with aluminum still partially oxidized. The passivating layer on Ti6Al4V alloy was thicker than Ti2 alloy.

Fig. 5,*c* shows the wide angle scan for Ti15Mo alloy. The spectra was predominately TiO_2, with smaller contributions from the sub-oxides and oxides of Mo. Various oxides and sub-oxides of Mo were present on the surface but only +2 and +6 oxidation states were detectable and the bulk composition was visible only after ~42 nm of the surface removal.

The thickness values of the alloys follows the order Ti15Mo > Ti6Al4V > Ti2. Ca, P and N were also detected on all the alloys investigated. Ca and P have their origin from the cell culture medium as it is known that these elements are present over the samples following immersion into SBF or HBSS which has already been demonstrated by several researchers [32–35]. Another source of Ca and P is related to the extracellular matrix formation by the bone forming cells. It was shown by SEM observations of such a substrate cell interface that Ca and P globular deposits are produced by the cells as soon as they colonize the material substrate [32–35].

High-resolution surface profiles were acquired for C 1s, O 1s, Ti 2p, P 2p and Ca 2p present over the alloy samples. They provided an indication of the chemical composition of calcium phosphate and titanium oxide formed on their surfaces. The high-resolution spectra were very similar for all the alloys tested. The binding energies obtained differed by a maximum of ± 0.2 eV.

Fig. 6 shows the high resolution surface spectrum for C 1s. The spectrum dominates by a shoulder at high energy and it is necessary to employ two peaks to achieve the best fit. The main peak has a BE of 288.2 ± 0.1 eV, which indicates that the carbon is bonded to O or other hydroxyl groups [34]. The full width half maximum (FWHM) of the order of 2.7 eV for the lower binding energy peak and 2.5 eV for the higher BE peak, suggests that there are overlapping peaks. Therefore, carbon may be present as a mixture of compounds, probably as sodium or calcium carbonates present in the cell culture since C 1s shows standard binding energies for these compounds of 289.4 eV and 289.8 eV, respectively [31]. C bonded to O or hydroxyl can also have contributions from other organic molecules present in the culture media.

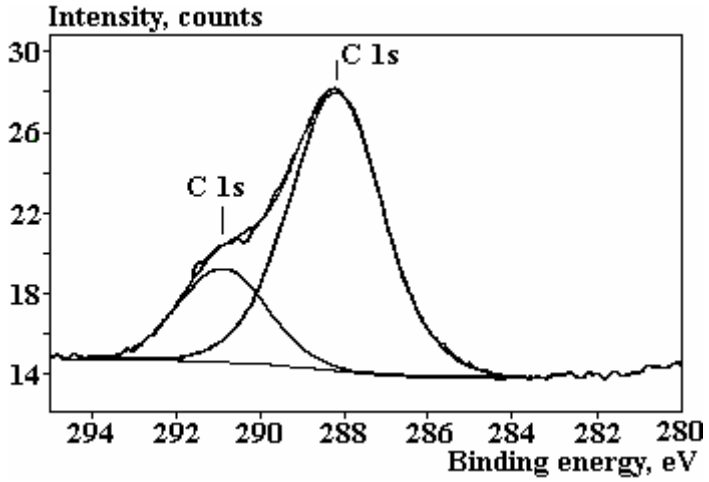

Fig. 6. High resolution XPS spectrum for C 1s

Fig. 7 shows the high resolution surface spectrum for O 1s. The primary peak has a BE of 534.6 eV and a FWHM of 2.73 eV, which indicates, as for the C 1s peak, the overlapping of more than one peak. A shoulder at lower BE (531.2 eV) is also detected. Armstrong et al. [36] determined the standard O 1s for TiO_2 at 533.3 eV, which is similar to the BE of the main peak. Binding energy differences between two major transitions can also indicate the chemical composition of a metal oxide. By calculating the energy difference between O 1s and Ti $2p_{3/2}$, ΔBE = O (1s) – Ti ($2p_{3/2}$) = 75.1 eV, which, according to the data obtained by the same authors, corresponds to TiO (+2 oxidation state). On the other hand, high-resolution spectra obtained by other researchers [33–34, 37–39] suggest that the BE for the oxide appears in the low-

energy range (~531 eV) followed by other components at higher BE, namely hydroxide/hydroxyl groups, phosphate or chemisorbed water. Taking this into account, it is possible that titanium oxide contributes mainly to the O 1s peak at BE 531.2 eV, and that the main peak at 534.6 eV can be mostly attributed to the presence of phosphates and adsorbed water. Recalculating Δ BE, one obtains the value of 71.7 eV, which is closer to the values obtained by Armstrong et al. [36] for TiO_2. The analysis of the Ti 2p spectra also suggests that titanium is mostly present in the form of TiO_2.

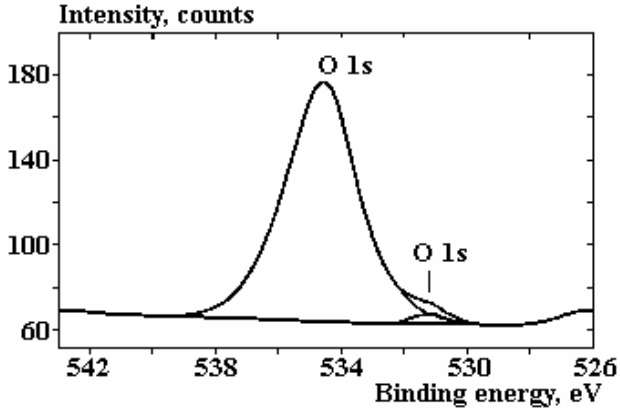

Fig. 7. High resolution spectrum for O 1s

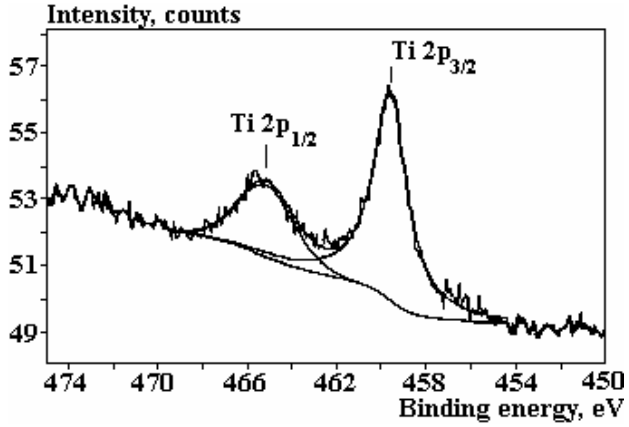

Fig. 8. High resolution spectra for Ti 2p

Fig. 8 shows the high resolution surface spectrum for Ti 2p. The Ti 2p peak is a doublet peak, Ti $2p_{3/2}$ at 459.5 ±0.1 eV and Ti $2p_{1/2}$ at 465.0 ± 0.2 eV. This indicates that titanium is present mainly in the oxide state [30] and by taking into account the BE of the peaks [31, 37] and the separation between them [31], it is evident that the oxide present is TiO_2, which is in accordance with results from the O 1s spectra. Some contributions from other oxidation states were detected between the main peak and 454.0 eV, which is the BE value for Ti metal. This suggests that the surface oxide film was too thick to allow photo-electrons from the bulk metal to reach the surface.

Fig. 9 shows the high resolution surface spectrum for P 2p. This is a single peak with a BE of 136.0 ±0.1 eV and a FWHM of 2.39 eV, indicating a probable overlapping peak.

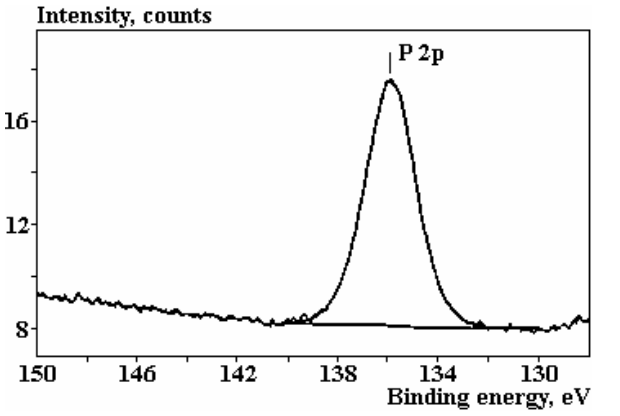

Fig. 9. High resolution spectra for P 2p

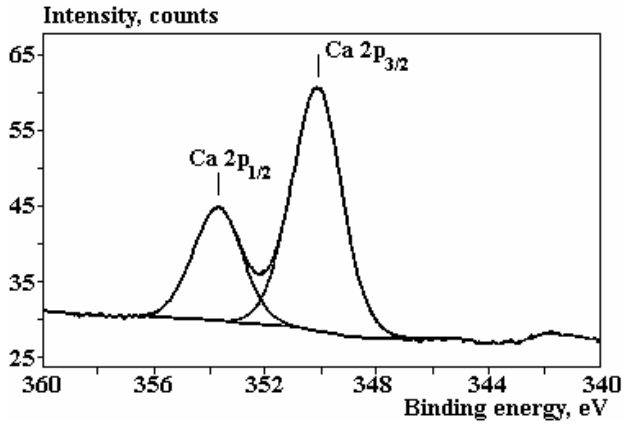

Fig. 10. High resolution spectra of Ca 2p

Fig. 10 shows the high resolution surface spectrum for Ca 2p. This is again a doublet peak with Ca $2p_{1/2}$ at 353.8 ± 0.1 eV and Ca $2p_{3/2}$ at 350.2 ± 0.1 eV. The FWHM of Ca $2p_{3/2}$ is around 2.1 eV, which is relatively large for Ca, which has a value of 1.68 eV [30]. This suggests that the peak overlaps with other contributions. Comparison of the energies of P 2p and Ca $2p_{3/2}$ suggests that a Ca and P compound may have been formed, probably a calcium hydrogen phosphate/calcium ortho phosphate or some other form of an apatite [40–43].

It is possible that the features obtained in the XPS spectra for Ca and P are mainly a consequence of the Ca and P rich globular deposits formed by the bone forming cells. As mentioned above, it is also possible that an apatite (some form of calcium ortho phosphate) may have been formed as a result of the immersion of the samples in the cell growth media composed of compounds of Ca and P. A third possibility could be the synergism of osteoblastic activity and cell culture growth media.

Amongst the alloys investigated, the anodized Ti15Mo β alloy displayed the presence of mixed oxides of Ti and Mo over its surface with the highest thickness value, thus promoting better osteoblast cell attachment and healthy cell morphology.

Conclusions

Anodization treatment employed has resulted in the formation of mixed oxides over titanium alloys. Ti15Mo alloy showed the thickest oxide, which was predominantly TiO_2 but also showed contributions from other oxidation states of Ti and Mo. Ti15Mo also showed the highest cell counts over its surface. Ti2 alloy demonstrated the presence of only titanium oxides and the mixed alloy showed contributions from Al, also.

Cell count values in conjunction with XPS results suggest that the presence of oxides and the biologically or chemically formed apatites that get adsorbed onto the oxide govern the cellular adhesion of osteoblast cells over an alloy surface. The highest cellular attachment of osteoblast cells over the Ti15Mo β alloy suggests that these oxides are playing a crucial role in the cellular processes in bringing about better osteointegration and implant performance.

REFERENCES

1. Wang K. The use of titanium for medical applications in USA. *Materials Science and Engineering A.* 1996, **213**, 134–137.
2. Lopez M.F., Jimenez J.A., Gutierreze A. Corrosion study of surface modified vanadium free titanium alloys. *Electrochimica Acta*. 2003, **48,** 1395–1401.
3. Milosev I, Metikos-Hukovic M, Strehblow H.H. Passive film on orthopaedic TiAlV alloy formed in physiological solution investigated by X-ray photoelectron spectroscopy. *Biomaterials*. 2000, **21**,2103–2113.
4. Rao S, Ushida T, Tateishi T, Okazaki Y, Asao S. Effect of Ti, Al and V ions on the relative growth rates of fibroblasts and osteoblat cells. *Bio-Medical Materials Engineering.* 1996, **6**, 79–86.
5. Schmidt H, Exner H.E., Ruck D.M., Angert N, Fink U. *Advances in material science and implant orthopaedic surgery.* edited by Kossowsky R, Kossowsky N, NATO-ASI series E: Applied Science. 1995, **24**, 207–221.
6. Leitao E, Sa C, Silva RA, Barbosa MA, Ali H. Electrochemical and surface modifications on N+-ion implanted Ti6Al4V immersed in HBSS. *Corros. Sci*. 1995, **37**, 1861.
7. Davies J.E., Ottensmeyer P., Shen X., Hashimoto M., Peel SAF, Early extracellular matrix synthesis by bone cells. *In: Davies JE, ed. The bone/biomaterial interface.* University of Toronto Press, 1991. 214–228.
8. Gomi K., Davies J.E. Guided bone tissue elaboration by guided cells. *J. Biomedical Mater. Res*. 1993, **27**, 429.
9. Gomi K., de Bruijn J.D., Ogura M., Davies J.D. Osteoclastic resorption of calcium phosphate coatings applied with electrostatic spray deposition. *Cells and Mater*. 1993, **3,** 151.
10. Martin JY, Schwartz Z, Hummert TW, Schraub DM, Simpson J, Lankford J, Dean DD, Cochran DL, Boyan BD.Effect of titanium surface roughness on proliferation, differentiation and protein synthesis of human osteoblast like cells. *J. Biomedical Mater.* 1995, **29**, 389.
11. Schreiber BG, Tuan RS. Enhanced extracellular matrix production and mineralization by osteoblasts cultured on titanium surfaces in vitro. *J. Cell Sci*. 1992, **101**, 209.
12. de Brujin J.D., Klein CPAT, de Groot K.K., Van Blitterswijk C.A. Influence of crystal structure on the establishment of the bone calcium phosphate interface in vitro. *Cells and Mater.*1993, **3**, 407–417.
13. de Brujin J.D., Klein CPAT, de Groot K.K, Van Blitterswijk C.A. Influence of crystal structure on the establishment of the bone calcium phosphate interface in vitro. *Cells and Mater.*1993, 3, 407.
14. Orr R.D., de Bruijn J.D., Davies J.D. Scanning electron microscopy of the bone interface with titanium, titanium alloy and hydroxyapatite. *Cells Mater*. 1992, **2**, 241–251.
15. Banerjee R, Nag S, Stechschulte J, Fraser HL. Strengthening mechanisms in Ti-Nb-Zr-Ta and Ti Mo-Zr-Fe orthopaedic alloys. *Biomaterials.* 2004, **25**, 3413–3419.
16. Nag S, Banerjee R, Stechschulte J, Fraser H.L. Comparison of microstructural evolution in Ti-Mo-Zr-Fe and Ti-15Mo biocompatible alloys. *Journal of Materials Science: Materials in Medicine*. 2005, 16, 679–685.
17. Nag S., Banerjee R., Fraser H.L. Microstructural evolution and strengthening mechanisms in Ti-Nb-Zr-Ta, Ti-Mo-Zr-Fe and Ti-15Mo biocompatible alloys. *Materials Science and Engineering C*. 2005, **25**, 357–362.
18. Brunette D.M., Tengvall P., Textor M., Thomsen P. *Titanium in Medicine: Material Science, Surface Science, Engineering, Biological Responses and Medical Applications*. Springer, 2001.
19. Karthega M, Raman V, Rajendran N. Influence of potential on the electrochemical behavior of β titanium alloys in Hanks solution. *Acta Biomaterialia*. 2007, **3,** 1019–1023.
20. Lavos-Valereto C., Wolynec S., Ramires I., Guastaldi A.C., Costa I. Electrochemical impedance spectroscopy characterization of passive film formed on implant Ti–6Al–7Nb alloy in Hank's solution. *J. Mater. Sci.: Mater Med.* 2004, **15**(1), 55–59.

21. Jablokov V.R., Nutt M.J., Richelsoph M.E., Freese H.L. The Application of Ti-15Mo Beta Titanium Alloy in High Strength Structural Orthopaedic Applications. *J of ASTM International*, 2005, **2**(8), 83–100.
22. Zardiackas L.D., Mitchell D.W., Disegi J.A. *Medical Applications of Titanium and Its Alloys: The Material and Biological Issues*. ASTM STP1272, ASTM International. West Conshohocken, PA. 1996. 60–75.
23. Bogan J., Zardiackas L., Disegi J.A. Stress Corrosion Cracking Resistance of Titanium Implant Materials. *27th Annual Meeting of the Society for Biomaterials*. St. Paul MN: 24–29 April 2001.
24. Bhola SM, Bhola R, Mishra B, Olson DL. Electrochemical impedance spectroscopic characterization of the oxide film formed over low modulus Ti–35.5Nb–7.3Zr–5.7Ta alloy in phosphate buffer saline at various potentials. *J. Material Science.* 2010, **45**(22), 6179.
25. Bhola R, Bhola SM, Ayers R, Mishra B, Olson Dl, Ohno T. Electrochemical Characteristics of Titanium and its alloys in Phosphate Buffer Saline. *Medical Device Materials V. Proceedings from the Materials & Processes for Medical Devices Conference 2009*, J. Gilbert, Ed. (Minneapolis, MN), ASM International, August 10–12, 2009.
26. Black J. *In Biological Performance of Materials: Fundamentals of Biocompatibility.* New York: Marcel Decker Inc., 1992.
27. Bhola R, Bhola SM, Ayers R, Mishra B, Olson DL, Ohno T. Cellular response of titanium and its alloys as implants. *J. Oral Implantol*. 2010, doi: 10.1563/AAID-JOI-D-09-00075.1.
28. Walker PR, Leblanc J, Sikorska M. Effects of aluminum and other cations on the structure of brain and liver chromatins. *Biochemistry.* 1990, **28**, 3911–3915.
29. Yumoto S, Ohashi H, Nagai H, Kakimi S, Ogawa S, Iwata Y. Aluminium neurotoxicity in the rat brain. *International Journal of PIXE*. 1992, **2**, 493–504.
30. Puleo DA, Huh WW. Acute toxicity of metal ions in cultures of osteogenic cells derived from bone marrow stromal cells. *J. Appl. Biomater* 1995, 6, 109.
31. Ikeo N, Iijima Y, Niimura N, Sigematsu M, Tazava T, Matsumoto S, Kojima K, Nagasawa Y. *Handbook of X-ray photo-electron spectroscopy.* JEOL. 1991.
32. Hanawa T, Ota M. Calcium phosphate naturally formed on titanium in electrolyte solution. *Biomaterials* 1991, 12, 767.
33. Hanawa T. *Proceedings of the Bone-Biomaterial Interface Workshop*, December 1990, edited by J.E. Davies (Univ. Toronto Press, 1991), pp. 49–61.
34. Hanawa T., Ota M. Characterization of surface film formed on titanium in electrolyte using XPS. *Appl. Surface Sci* 1992, **55**, 269.
35. Leitao E., Barbosa M.A., de Groot K. In vitro calcification of orthopaedic implant materials. *J. Mater. Sci. Mater. Med.* 1995, 6, 849.
36. Armstrong NR, Quinn RK. Auger and X-ray Photoelectron Spectroscopic and Electrochemical Characterization of Titanium Thin Film Electrodes. *Surface Sci,* 1977, **67**(2), 451–468.
37. Lausmaa J., Kasemo B., Mattsson H. Surface spectroscopic characterisation of titanium implant materials**.** ***Appl. Surf. Sci.*** 1990**, 44**, 133**–**146.
38. Ong JL, Prince CW, Lucas LC. Cellular response to well-characterized calcium phosphate coatings and titanium surfaces in vitro. *J. Biomed. Mater. Res*. 1995, **29**, 165.
39. Thompson GJ and Puleo D.A. Effects of Subletal Metal-Ion Concentrations on Osteogenic Cells Derived from Bone-Marrow Stromal Cells. *J. Appl. Biomater*. 1995, **6**(4), 249–258.
40. Vanzillotta P.S., Sader M.S., Bastos I.N., de A. Soares G. Improvement of in vitro titanium bioactivity by three different surface treatments. *Dental Materials*. 2006, 22, 275–282.
41. Chusuei C.C., Goodman D.W. Calcium Phosphate Phase Identification Using XPS and Time-of-Flight Cluster SIMS. *Anal. Chem.* 1999, **71**, 149–153.
42. Demri B., Muster D. XPS study of some calcium compounds. *Journal of Materials Processing Technology*. 1995, **55**, 311–314.
43. Regi M.V., Pariente J.P., Barba I.I., Salinas A.J. Compositional variations in the calcium phosphate layer growth on gel glasses soaked in a simulated body fluid. *Chem. Mater*. 2000, **12**, 3770–3775.

Received 10.02.11

Summary

The cellular response of anodically treated titanium alloys was investigated using cell attachment, morphological and surface analytical techniques. The behavior of a β Ti15Mo alloy has been compared with the conventional mixed alloy, Ti6Al4V and the α alloy, Ti2. Ti15Mo β alloy demonstrated a higher cell count and a thicker oxide on its surface. The presence of Ca and P was detected in all the alloys after the invitro cell culture test. TiO_2 was present as the dominant oxide in all three alloys.